

The effect of pressure on block copolymer micelle formation: fluorescence and light scattering studies of poly(styrene-*b*-ethylene propylene) in heptane

D. A. Ylitalo and C. W. Frank*

Department of Chemical Engineering, Stanford University, Stanford, CA 94305-5025, USA

(Received 6 November 1995; revised 28 December 1995)

Pressure dependent excimer fluorescence and dynamic light scattering measurements are made on poly(styrene-*b*-ethylene propylene) (PSPEP) diblock copolymers that form micelles in the selective solvent *n*-heptane. We determine the critical micelle temperature (cmt) as a function of block copolymer concentration and applied pressure up to 200 MPa by monitoring the excimer emission band energy, which passes through a minimum at the cmt. The photophysical determination of cmt agrees with simple turbidity measurements taken under the same conditions. The hydrodynamic radius, as determined by dynamic light scattering, increases approximately 5% for a PSPEP diblock copolymer having PS $M_w = 35\,000$ and PEP $M_w = 61\,000$, denoted PSPEP 35/61, with increasing pressure. At 298 K, the hydrodynamic radius decreases approximately 4% for the PSPEP diblock copolymer with PS $M_w = 21\,000$ and PEP $M_w = 66\,000$, denoted PSPEP 21/66. These size changes are consistent with a negative volume change upon micellization for PSPEP 35/61 and a positive value for PSPEP 21/66. For temperatures greater than 308 K, both block copolymers exhibit positive volume changes upon micellization. Using a simple corresponding states thermodynamic model, we relate the pressure effects to a decrease in the PS/heptane interaction parameter, i.e. an increase in the solvent quality with increasing pressure. Copyright © 1996 Elsevier Science Ltd.

(Keywords: block copolymer micelle; pressure; excimer fluorescence)

INTRODUCTION

Micelle formation by block copolymers in solvents selective for one block has been the subject of much study over the past two decades^{1–13}. The effects of temperature, concentration, and solvent have been analysed both experimentally^{1–10} and theoretically^{11–13} to provide insight to the micellization process. For a particular block copolymer molecular weight and architecture, the solution exhibits a critical micelle concentration (cmc) at a fixed temperature and pressure, above which the block copolymer will aggregate to form micelles consisting of a dense core of the insoluble block and an expanded, solvated shell of the soluble block. Since the driving force behind this aggregation is a negative enthalpy of micellization^{5,14}, there is also a critical micelle temperature (cmt) at a fixed concentration and pressure, above which the micelles dissolve and the block copolymers exist entirely as dispersed chains.

Pressure has been an under-utilized thermodynamic variable in the study of block copolymer micelle formation, in spite of relevant applications. For example, micelle-forming block copolymers are added to lubricating oils as viscosity modifiers¹⁵. The

performance of such a lubricant is strongly affected by the response of the micelle to the locally high pressures found under heavy load conditions. Moreover, the response of the micelles to applied pressure can provide fundamental information about the factors that affect micellization. In fact, we expect there to be a critical micelle pressure (cmp) corresponding to a particular concentration and temperature. Whether application of pressure causes micelle formation or dissolution will depend upon the sign of the volume change upon micellization, ΔV_{mic} : for a negative ΔV_{mic} , micelle formation will be promoted by application of pressure; for a positive ΔV_{mic} , increasing pressure causes micelle destabilization. In this study, we utilize static and dynamic light scattering and excimer fluorescence techniques to further our understanding of the thermodynamics and structure of block copolymer micelles under pressure.

Pioneering light scattering studies on the effect of pressure on homopolymers in solution were performed over two decades ago by Schulz and Lechner^{16,17}. They discussed the effect of pressure on the radius of gyration and second virial coefficient, A_2 , in terms of excluded volume theory. Patterson^{18,19} later extended the work of Prigogine²⁰ to calculate the pressure dependence of the Flory–Huggins χ interaction parameter in terms of a corresponding states treatment. This

* To whom correspondence should be addressed

approach accounted for a non-combinatorial entropy contribution, which arose due to differences in free volume between the solvent and the polymer; application of pressure generally decreases the free volume of a solvent much more than that of a polymer. McDonald and Claesson²¹ made comparisons between the theory and light scattering measurements of A_2 in dilute solutions of polystyrene (PS) up to 200 MPa. They qualitatively predicted positive as well as negative dependence of A_2 on pressure for five different solvents, thus validating the corresponding states approach for describing pressure effects.

The effect of pressure on the hydrodynamic properties of homopolymers in solution has also been studied. Roots and Nystrom²², and Freeman *et al.*²³ have performed dynamic light scattering measurements on toluene solutions of PS at elevated pressures. The hydrodynamic radius of the polymer coil was unchanged by pressures up to 5000 atm, in contrast to static light scattering results that indicated up to a 12% decrease in the radius of gyration. No explanation for the difference in pressure sensitivity between the hydrodynamic radius and the radius of gyration was given.

In previous work on the concentration and temperature dependence of the poly(styrene-*b*-ethylene propylene) (PSPEP) system at atmospheric pressure, Yeung and Frank⁵ utilized dynamic light scattering and the PS excimer emission energy and bandwidth to monitor both the global micellar morphology as well as the state of the PS block in the PSPEP micelle core. In the present paper, we extend this work to monitor the critical micelle transitions as a function of applied pressure. We report photophysical measurements only on the excimer emission energy, however, as the excimer bandwidth is sensitive to changes in dissolved oxygen content that cannot be easily controlled in the high pressure cell. As a complement to the localized information provided by the photophysical measurements, we also determine the cmt from the minimum in the 90° scattered light intensity. Moreover, we use dynamic light scattering to determine micelle size and its dependence on pressure. Finally, we interpret the resulting composition-temperature-pressure phase diagrams in terms of an equation-of-state treatment that considers only enthalpic interactions between the polystyrene core of the micelle and the surrounding heptane solvent.

EXPERIMENTAL

Materials and preparation

The poly(styrene-*b*-ethylene propylene) diblock copolymers were provided by Shell Development Co. The styrene/ethylene propylene molecular weights were $M_w = 35\,000/61\,000$ and $21\,000/66\,000$ for the samples denoted as 35/61 and 21/66, respectively. The overall polydispersity of each sample was 1.02, as determined by gel permeation chromatography. Before use, the polymer was subjected to several cycles of precipitation from tetrahydrofuran into methanol or acetone to remove any traces of PS homopolymer, if present, and added stabilizers. The solvent was spectro-grade *n*-heptane (Burdick & Jackson), a non-solvent for PS, which was used as received.

Heptane solutions of several concentrations were prepared in cylindrical quartz cuvettes. In every case,

the concentrations were above the cmc of ≈ 0.001 wt%, but below 0.75 wt% where intermicellar effects begin to play a significant role, as evidenced by the bimodal relaxation time distribution function for the dynamic light scattering⁵. Each sample was subjected to five freeze-pump-thaw cycles to remove dissolved oxygen, which is an efficient quencher of PS fluorescence, and then vacuum sealed at less than 2×10^{-5} torr. The sealed tubes were kept at 150°C for 6 h to ensure complete dissolution and then slowly cooled to room temperature over 8 h. This thermal treatment produced a consistent, apparently equilibrium micelle structure, from which no appreciable changes in micelle size or fluorescence spectra were observed after storing at room temperature for several weeks.

Photophysical and light scattering measurements

Pressure control. The samples were checked for fluorescence impurities while still in the quartz tubes, after which the tubes were opened under a nitrogen atmosphere and the samples loaded into the high pressure optical cell. The four-port pressure cell, which has been described elsewhere²⁴, was configured with three single crystal sapphire windows to allow for simultaneous 90° fluorescence and 90° light scattering. A thermocouple was placed in the remaining port and temperature was controlled within 0.2°C with a thyristor thermostat connected to a set of resistance heaters located outside the cell. In each set of experiments the pressure was increased to the desired value with a pressure generating system that has been described elsewhere²⁴. Fluorescence and static light scattering measurements were taken at 2–7°C intervals with 45 min to 1 h equilibration time between data points. Similar experiments were performed with 20 min and 1.5 h equilibration times at 1350 atm. In each case, the fluorescence data agreed with experimental error, leading us to believe that we had achieved thermodynamic equilibrium with our 45 min equilibration time. Experiments were also run by decreasing the temperature from above the cmt, and no change in the measured cmt was observed.

Excimer fluorescence. The spectrofluorometer has been previously described¹⁵. The spectra were first corrected for instrument response and to remove the Raman scattering peak of the solvent. The corrected spectra were transformed to an energy scale and then resolved into a monomer and an excimer peak. We assumed the shape of the PS monomer peak to be that of *sec*-butyl benzene in heptane with an allowance for spectral red-shift as the pressure was increased. The excimer peak was assumed to be Gaussian on an energy scale. A Levenberg-Marquardt non-linear regression routine was used to deconvolute the peaks, and goodness-of-fit was based on inspection of the weighted residuals and analysis of variance.

Static light scattering. Concurrent with the excimer fluorescence measurements, we performed total intensity light scattering with 600 nm incident light. The intensity of the light scattered at 90° was ratioed to a reference channel proportional to the incident light intensity. This ratio is proportional to the Rayleigh ratio at 90° and, thus, is related to the molecular weight and concentration of micelles present in the scattering volume²⁵.

Dynamic light scattering. The dynamic light scattering experiments were performed with a Brookhaven photon correlation system having a Lexel 95-2 2 W argon-ion laser (514.5 nm line), Brookhaven BI-200 goniometer and Brookhaven BI-2030 136 channel correlator. To accommodate the high pressure optical cell, an alternate light collection system was devised that consisted of a four inch tube mounted perpendicular to the wall of the pressure cell with 0.5 mm pinholes at each end to select the appropriate scattered light. The Brookhaven photomultiplier tube was then placed at the end of the tube, supported and sealed from stray light. The mean temperature was 21.4°C and fluctuations did not exceed 0.2°C.

PSPEP samples of 0.1 wt% in heptane were loaded into the pressure cell after being filtered through a 0.45 μ filter. The cleanliness of the sample could be checked by monitoring the agreement between the measured and calculated correlation baselines provided by the Brookhaven data acquisition program. The measured baseline was obtained from the average of the long-time delay channels collected by the correlator, and the calculated baseline was obtained from the average intensity. At least eight runs were made under each set of conditions for which the measured and calculated baselines agreed within 0.1%. The hydrodynamic radius was measured before pressurization, and then the pressure was increased by forcing additional filtered solvent into the high pressure cell by means of a screw pump. The pressure was measured with a Bourdon tube gauge connected to the high pressure line.

Data from the Brookhaven correlator were collected by an IBM AT computer, and a cumulant analysis was performed. The data accepted based on baseline agreement were then transferred to a DEC 3100 workstation for analysis by the CONTIN inversion program provided to us by Provencher^{26,27}. This program yields smooth distributions of decay rates from the autocorrelation function. We prefer CONTIN for inverting dynamic light scattering data because of its ability to penalize irregular distributions and its ability to factor out background scattering from dust. In our experiments, the dust term calculated by CONTIN was acceptable only when equal to zero. In the event that a bimodal solution was obtained, the peak around 3–7 nm was disregarded and the main peak was taken to represent the micelles.

Dynamic light scattering measurements were made from the highest to the lowest pressure with one to three hours of equilibration between experiments. A check of equilibration was made by increasing the temperature above the cmt to dissolve the micelles and then cooling slowly to room temperature at a pressure of 70 MPa. Agreement between the measurements before and after dissolution was well within the experimental error for the 21/66 block copolymer. The 35/61 block copolymer, however, exhibited a larger hydrodynamic radius before dissolution than after. For this reason, the sample was brought above its cmt at each pressure and then cooled to room temperature before measurement. A final measurement of the hydrodynamic radius at atmospheric pressure was made at the end of the experiment to check against the initial value. In each experiment, the agreement between the initial and final values was within 0.5%.

The hydrodynamic radius of the micelles is determined from the distribution of decay rates, $G(T)$, calculated by

Table 1 Micelle characteristics at atmospheric pressure

Polymer	$\langle R_h \rangle$ (nm)	$[\eta]$ (cm ³ g ⁻¹)	N_{agg}
21-66	44.8	85	76
35-61	46.8	65	103

the CONTIN program. The decay rate, Γ , is related to the translational diffusion coefficient, D , by $\Gamma = q^2 D$, where q is the scattering vector defined as $4\pi n \sin(\theta/2)/\lambda$. We then use the Stokes-Einstein relation for non-interacting particles to obtain the distribution of hydrodynamic radii, $R_h = kT/6\pi\eta D$, which is then averaged over the whole distribution to give the average hydrodynamic radius, $\langle R_h \rangle$.

RESULTS

Light scattering measurements of micelle size

Dynamic light scattering and intrinsic viscosity measurements were combined to determine the hydrodynamic radius and aggregation number for each block copolymer; the results are shown in *Table 1*. The aggregation number was calculated from equation (1), which Tuzar⁷ has noted is applicable for block copolymer micelles.

$$[\eta] = \frac{10\pi R_h^3 N_{AV}}{3M_m} \quad (1)$$

where M_m is the micellar mass and $[\eta]$ is the intrinsic viscosity. As the size of the insoluble block is increased, the micelles formed have a larger aggregation number and a larger hydrodynamic radius. These results agree with those of Bahadur *et al.*² who studied micelles of poly(styrene-*b*-isoprene) in heptane and dodecane. As the insoluble PS block length was increased, while keeping the polyisoprene block length constant, the hydrodynamic radius increased, the intrinsic viscosity decreased, and the aggregation number increased, all in agreement with our results. This is to be expected based purely on a geometric argument; the more asymmetric block copolymer (21/66) should have a lower aggregation number due to the crowding of chains in the corona.

To establish the effect of pressure on the micelle size, dynamic light scattering measurements were made from 0.1 to 150 MPa for both block copolymers. The relative average hydrodynamic radii for each polymer, as determined by the CONTIN analysis program, are plotted against pressure in *Figure 1*. For the 35/61 block copolymer, an increase in pressure increases the hydrodynamic radius by approximately 6%, while an approximately 4% decrease in the hydrodynamic radius is observed for the 21/66 copolymer in the same pressure region. In addition, the intensity distributions were up to 40% broader than the distributions at atmospheric pressure. Because the solvent is much more compressible at the lowest pressures, the greatest effect is observed with the initial increase in pressure.

Fluorescence measurements of the micelle phase diagram

An important aspect of this work is the establishment of the complementarity of light scattering and fluorescence methods for the study of block copolymer micelle structure over a wide range of distance scales. Our first

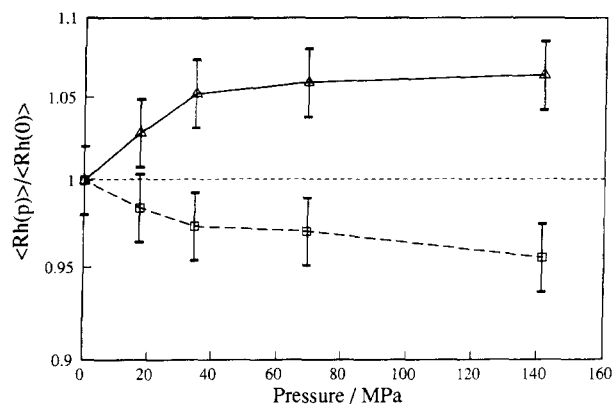


Figure 1 Pressure dependence of the normalized average hydrodynamic radius of the PSPEP 35/61 (Δ) and PSPEP 21/66 (\square) micelles for 0.1 wt% heptane solution at 21°C. Error bars indicate uncertainty in solvent viscosity and refractive index; actual experimental standard deviations are approximately 1%

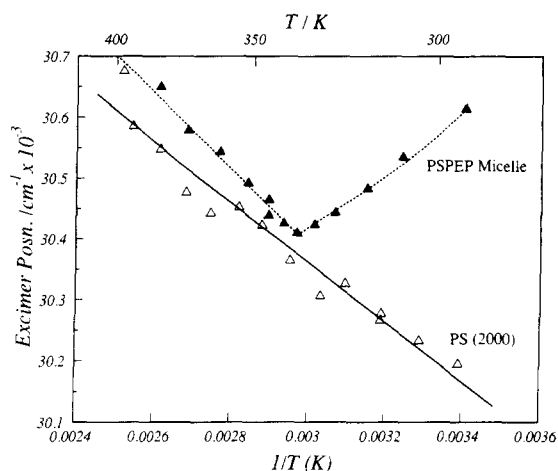


Figure 3 Temperature dependence of the excimer emission band position for PS ($M_w = 2000$) (Δ) and PSPEP 35/61 (\blacktriangle) at 35 MPa

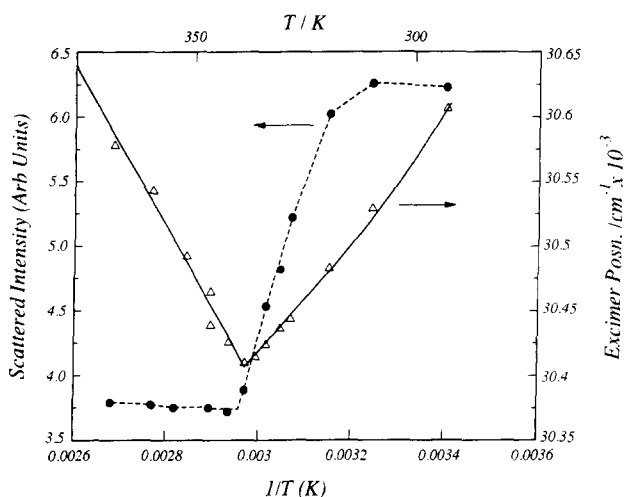


Figure 2 Comparison of temperature dependence of excimer emission band position and static 90° scattered light intensity for 0.045 wt% PSPEP 35/61

indication that such a correlation exists is given in *Figure 2*, which shows the temperature dependence of the scattered light intensity at 600 nm along with the excimer emission energy for the 0.045 wt% PSPEP 35/61 block copolymer solution at 35 MPa. The initial increase in temperature does not appreciably change the scattered intensity, while the excimer emission energy steadily decreases. In this region we believe that the core of the micelle is being imbibed with solvent, consistent with n.m.r. data of Candau³ and our previous PSPEP micelle excimer data at atmospheric pressure⁵. We identify the temperature at which the static light scattering plateau is first reached as the cmt for this particular pressure and composition, i.e. this is a standard cloud point type of observation. At elevated pressures for the 35/61 micelles and for all pressures in the 21/66 micelles, the minimum in the excimer emission energy agreed with the cmt obtained from light scattering within 2°C. Because of the coincidence of the starting point of the static high temperature light scattering plateau and the minimum in the excimer band position, it is tempting to also conclude that the fluorescence spectral data reflect the same type of micellar transition. However, this conclusion requires careful validation, which we have done with an

appropriate reference compound study, as described in the following.

In order to provide a calibration for the pressure dependence of the photophysical behaviour of the PS block in PSPEP, we initially measured the fluorescence spectrum of a low molecular weight PS chain ($M_w = 2000$) that is sparingly soluble in heptane. While the PS(2000) chain will approximate the fluorescence characteristics of the PS block of the dispersed, solvated PSPEP chain, we expect that the configuration of PS(2000) will be more expanded than that of the PS block of the PSPEP block copolymer. Thus, the fluorescence characteristics may not be a precise match to the dispersed phase. We show in *Figure 3* the excimer position of a 0.045 wt% PSPEP 35/61 micelle solution and the PS(2000)/heptane solution as a function of temperature at 35 MPa. In the PSPEP solution at low temperatures, almost all of the block copolymer chains are incorporated in micelles and the excimer-forming-sites (EFS) are in the PS-rich micelle core. For this situation, the room temperature excimer emission energy is blue-shifted approximately 600–800 cm^{-1} from values seen in the PS(2000)/heptane solution where the EFS are substantially solvated by heptane. With increasing temperature, the excimer emission energy of the PSPEP solution red-shifts. By contrast, the excimer energy blue shifts as the temperature is increased for the PS(2000) solution, reflecting the changes in solvent density and refractive index on the excimer energetics²⁸.

These two sets of results suggest that the initial red shift in the excimer emission position for the PSPEP micelle solution is entirely due to the increased contact of the excimer forming sites in the PS core with the heptane solvent. The increased solvent contact is consistent with either a dissolution of micelles as the temperature increases or an increased solvent penetration into the micelle core, both of which are expected^{3,29}. Because the cmc increases as the temperature is increased, there will be a larger contribution to the fluorescence from the dispersed chains as the temperature is raised to the cmt. Thus, we interpret the point at which the excimer energy reaches a minimum to be the cmt. Above the cmt the temperature dependence of the excimer energy in the micelle solution mimics that of the low molecular weight PS(2000) in heptane. The small blue shift in position may reflect differences in chain conformation and the ability

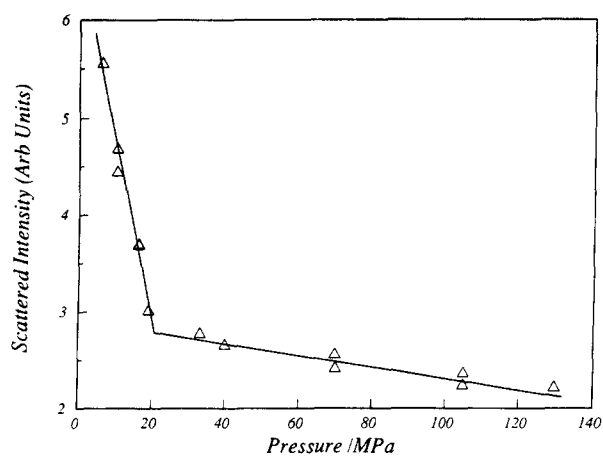


Figure 4 Pressure dependence of static 90° scattered light intensity for 0.5 wt% PSPEP 35/61 at 358 K

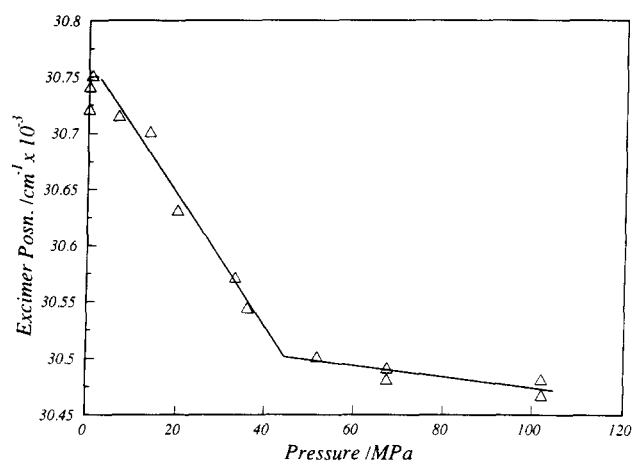


Figure 5 Pressure dependence of excimer emission band position for 0.5 wt% PSPEP 35/61 at 352 K

of the block copolymer to shield itself from the solvent. Indeed, the concept of a unimolecular micelle in which the collapsed PS block is enveloped by the PEP block is a widely proposed representation of the dispersed chain³⁰.

Although our ultimate objective is to present and interpret a complete concentration–temperature–pressure phase diagram for the PSPEP block copolymer, it is instructive to continue the examination of the dependence of light scattering and fluorescence observables on a single independent variable, i.e. pressure. We begin in Figure 4 with the simple turbidity measurement for a 0.5 wt% 35/61 PSPEP solution at 358 K, which is below the cmt at atmospheric pressure. By analogy with the temperature cloud point measurements, we assign the break in the scattered light intensity at about 20 MPa as the critical micelle pressure (cmp) for this concentration and temperature, above which the equilibrium is shifted toward the individual block copolymer molecules. For comparison, Figure 5 shows the pressure dependence of the excimer emission energy of a 0.5 wt% solution of 35/61 PSPEP at 353 K. These data reflect a shift in the micelle equilibrium towards free chains as the pressure is increased up to about 40 MPa, above which micelles cease to exist. The static light scattering and fluorescence data are similar but not identical due to the different temperatures. From Figures 2–5 we see that, for a given concentration, an increase in temperature has the same

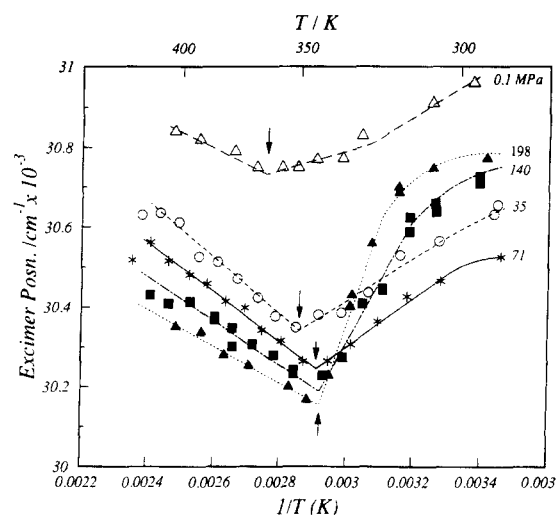


Figure 6 Temperature dependence of excimer emission band position for 0.5 wt% PSPEP 35/61 at several pressures. Arrows denote the critical micelle temperatures (cmt)

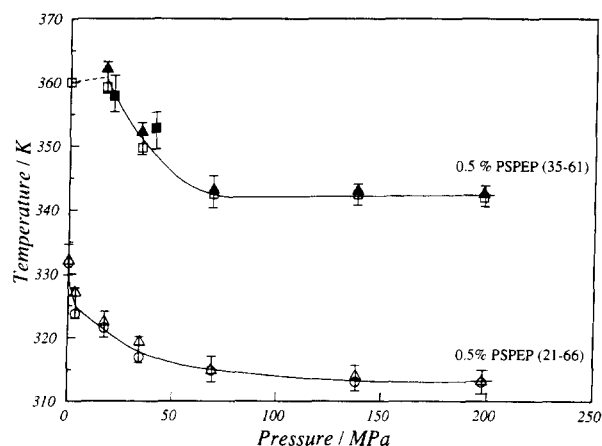


Figure 7 Temperature/pressure phase diagram for 0.5 wt% PSPEP 35/61 from excimer emission band position (□) and static 90° light scattering (▲) and for 0.5 wt% PSPEP 21/66 from excimer emission band position (○) and static 90° light scattering (△). Also shown are points from excimer emission band position and static 90° light scattering as a function of pressure

qualitative effect as an increase in pressure; both can cause micelle destabilization leading to the isolated copolymer molecules in solution.

At this point, the experimental results are sufficiently internally consistent to proceed with the use of the excimer emission band position as an empirical observable that is sensitive to the phase behaviour of the block copolymer. Figure 6 shows the temperature dependence of the excimer emission energy for several pressures at 0.5 wt% PSPEP 35/61 concentrations. Similar results were also obtained for the other concentrations studied and are not shown. As the pressure is increased, the cmt (denoted by the arrows), is shifted to lower temperatures. From atmospheric pressure to about 60–80 MPa the shift is approximately 15–20°C, but above that pressure the effect seems to have saturated. This effect is more easily seen in Figure 7, which illustrates the pressure–temperature boundary of the 0.5 wt% PSPEP solution for each of the block copolymers.

The phase boundary plots shown in Figure 7 also include points from the light scattering measurements

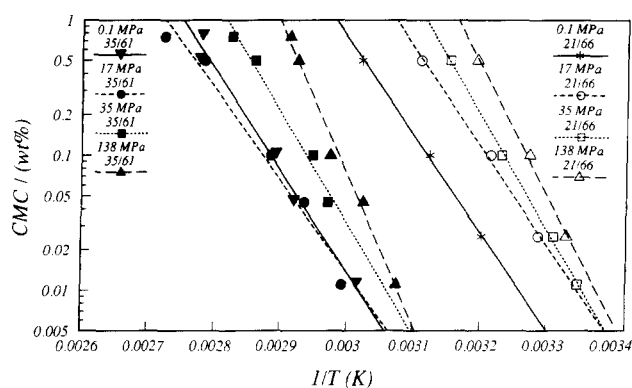


Figure 8 Temperature dependence of cmc for PSPEP 35/61 denoted by filled symbols and PSPEP 21/66 denoted by open symbols at several pressures

determined either by varying the pressure for constant temperature or by varying the temperature at constant pressure, and the agreement is excellent. This strongly suggests that our experimental procedure has achieved thermodynamic equilibrium. We did observe, however, that the cmt determined from the fluorescence method was consistently 0.5–2.0°C lower than that determined from light scattering measurements. This slight discrepancy results from the fact that the cmt is not a distinct transition; instead, the micelle volume fraction decreases steadily up to the cmt, where it vanishes. The light scattering technique is sensitive only to the micelles that still exist in solution, while the excimer emission energy reflects fluorescence from all chains, whether in micelles or in the dispersed phase. We note also that the light scattering technique could reflect loose aggregates of chains that are almost entirely solvated by the heptane solvent slightly above the cmt. Since the atmospheric pressure experiments for the 35/61 block copolymer did not show a discernible break in the light scattering data, we will not draw any conclusions about the data below 17 MPa for this block copolymer.

To obtain the full phase diagram for the PSPEP micelle system, we measured the pressure dependence of the cmt for several concentrations of block copolymer from 0.01 to 0.75 wt%, the results of which are shown in Figure 8. The data have been measured using the excimer emission energy, but light scattering gives almost identical results. To summarize the phase diagram, micelles are formed at high concentrations and low temperatures, and pressure shifts the phase boundary to higher concentrations or lower temperatures.

DISCUSSION

Thermodynamics

While we have found no report on the pressure dependence of block copolymer micellization thermodynamics, pressure has been used as a thermodynamic variable in the micellization of surfactants in aqueous solution^{31–43}. In early studies, reviewed by Offen³⁹, the cmc was measured as a function of pressure to calculate the volume change on micellization, ΔV_{mic} . An increase in pressure between 0.1 and 100 MPa increased the cmc, or effectively forced chains from micelles into the dispersed phase, as is observed for the PSPEP/heptane system. At a pressure of 120–150 MPa, however, the cmc reached a maximum and then began to decrease as the

pressure was increased further. These results were interpreted as a positive ΔV_{mic} at low pressures such that the volume of a surfactant molecule in a micelle was greater than a similar molecule in the aqueous phase. The monotonically decreasing ΔV_{mic} at high pressures was thought to result from a larger compressibility of the micelle core relative to the individual chain³⁹. Tanaka *et al.* were able to directly measure the partial molar volume and the compressibility of a surfactant both in aqueous solution and in a micellar system and verified that the volume difference was indeed positive at low pressures and changed sign around 100 MPa³⁴.

Tuddenham and Alexander³² first calculated ΔV_{mic} from the pressure dependence of the cmc in 1962, and their simple thermodynamic treatment has been the basis for most subsequent calculations of ΔV_{mic} ^{33–38}. Their closed association model assumes that the micelles are formed in an equilibrium reaction between free chains and micelles of predominantly one aggregation number



where A_1 is the concentration of free chains and A_n is the concentration of micelles with an aggregation number of n . This assumption is supported in our PSPEP system by the narrow distribution of micelle sizes obtained from our previous work⁵. The equilibrium constant K , can then be represented by

$$K = \frac{\hat{a}_{A_n}}{(\hat{a}_{A_1})^n} \quad (3)$$

where a is the activity of the free chain (A_1) or micelle (A_n).

To ensure that the standard free energy properties are pressure independent, we modify the Tuddenham and Alexander approach and integrate the fugacities from the standard state to the pressure of interest, thus yielding a term similar to the Poynting factor for gases. This leads to the expression for ΔG^0

$$\frac{\Delta G^0}{n} = RT \ln([A_1]) - \frac{RT}{n} \ln([A_n]) - \int_1^p \left(\frac{V_{A_n}}{n} - V_{A_1} \right) dp \quad (4)$$

where the third term is the Poynting correction. For our block copolymer system where n is large (≈ 100), we can neglect the second term and $[A_1]$ can be taken as the cmc in a closed association process. Differentiating both sides and realizing that the standard free energy is defined at 1 atm and is therefore independent of pressure, we get

$$RT \frac{\partial}{\partial p} (\ln \text{cmc})_T = \Delta V_{\text{mic}} \quad (5)$$

where ΔV_{mic} is defined as

$$\Delta V_{\text{mic}} = \left(\frac{\partial}{\partial p} \right)_T \int_1^p \left(\frac{V_{\text{mic}}}{n} - V_{A_1} \right) dp \quad (6)$$

This relation is similar to the result of Tuddenham and Alexander, but in their final equation the average volume of micellization was replaced by the standard volume of micellization, ΔV_{mic}^0 , which is not a function of pressure and therefore cannot be used to characterize the changing volume of micellization at elevated pressures.

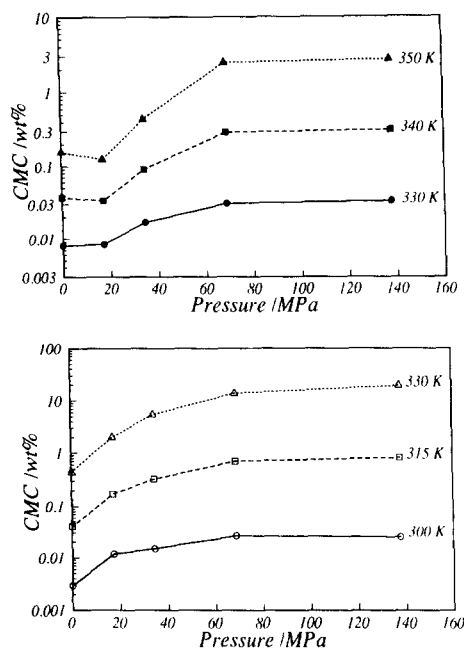


Figure 9 Pressure dependence of cmc for PSPEP 35/61 denoted by filled symbols and PSPEP 21/66 denoted by open symbols at several temperatures

Calculation of volume change upon micellization

In Figure 8 the cmt at a particular concentration reflects the temperature at which the bulk concentration is equal to the cmc, so our bulk concentrations are plotted on the ordinate as the cmc, and the respective cmt values are plotted on the abscissa. To quantify the effect of pressure on the thermodynamics of micellization, we calculate the volume change of micellization, ΔV_{mic} , from equation (5). To obtain the pressure dependence of the cmc at constant temperature required for equation (5), we take points from vertical lines drawn through the data in Figure 8. Figure 9 shows the pressure dependence of the logarithm of the cmc at three temperatures for each block copolymer, the slopes of each plot being proportional to ΔV_{mic} . Note that the cmc initially increases with pressure for PSPEP 21/66 at all temperatures. However, it decreases initially and then increases for PSPEP 35/61. From equation (5) this indicates that ΔV_{mic} is always positive for PSPEP 21/66 but is initially negative for PSPEP 35/61, subsequently becoming positive.

Table 2 is a collection of the ΔV_{mic} values calculated from the data in Figure 9 as well as representative values for a sodium dodecyl sulfate (SDS) surfactant in aqueous solution. Because of the problems with the data at atmospheric pressure for the 35/61 block copolymer, we tabulate ΔV_{mic} in the 17–35 MPa range as well as in the low pressure region. After normalization by the molar volumes of the PS block of our copolymer and the hydrocarbon tail of the SDS, we see that the ΔV_{mic} for the aqueous surfactant micelle system is substantially larger. This reflects the larger volumetric change that results from the transfer of a hydrocarbon chain from an aqueous environment to the hydrocarbon micelle core. We can also compare the micellization volumes for the two copolymer systems in the 17–35 MPa region. At the same temperature, the 21/66 block copolymer has a larger ΔV_{mic} than the polymer with the larger PS block.

Table 2 ΔV_{mic} values for PSPEP and SDS at various temperatures

Micelle system	T (K)	ΔV_{mic} ($\text{cm}^3 \text{mol}^{-1}$)	$\Delta V_{\text{mic}}/V_1$
PSPEP (35–61)/heptane	306	0	0
	17–35 MPa	330	3.4×10^{-3}
	17–35 MPa	340	4.9×10^{-3}
	17–35 MPa	350	6.4×10^{-3}
PSPEP (21–66)/heptane	280	0	0
	0–17 MPa	300	1.0×10^{-2}
	17–35 MPa		1.6×10^{-3}
	0–17 MPa	315	1.1×10^{-2}
	17–35 MPa		4.8×10^{-3}
	0–17 MPa	330	1.2×10^{-2}
17–35 MPa		8.0×10^{-3}	
SDS/ H_2O^b	298	11^a	5.9×10^{-2}
	313	10^a	5.4×10^{-2}

^a In the 0–30 MPa region

^b Data from ref. 21

Effect of pressure on polymer solution thermodynamics

In the literature on the effects of pressure on low molecular weight surfactant micellization, changes of solvent quality between the solvent and the surfactant have not been considered. In the case of polymer solutions, however, the large disparity in free volume between the polymer and solvent has an important effect on the resultant solution thermodynamics. Because the solvent is generally more compressible than the polymer, application of pressure should decrease the free volume effects and possibly decrease the χ parameter for the polymer/solvent system¹⁹. This is generally the case at high temperatures or in instances for which the free volume disparity is large. When free volume terms are less important, the application of pressure may then increase or decrease the χ parameter.

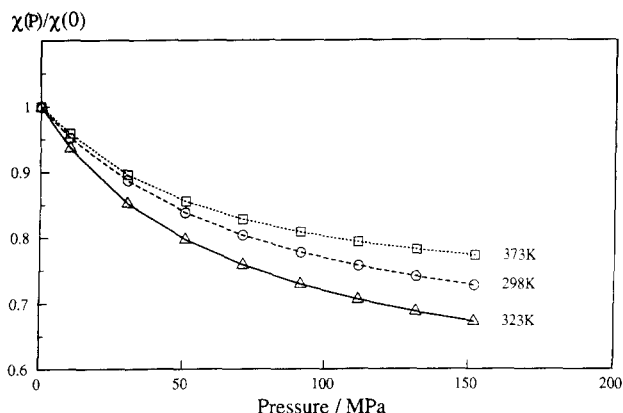
The Flory equation of state theory^{44–46} and Patterson's¹⁸ corresponding states theory for polymer solutions may be used to predict the effect of pressure on the χ parameter. Using the corresponding states treatment, McDonald and Claesson compared theoretical predictions to experimentally determined A_2 data for PS in several solvents between 0.1 and 500 MPa²¹. The theory was able to qualitatively describe the A_2 data for increases and decreases in pressure.

To simplify our discussion of the forces producing the decrease in cmt with pressure and the positive ΔV_{mic} in the block copolymer micelle system at higher pressures, we focus our attention on the polymer/solvent interactions that most strongly affect the micellization thermodynamics. The core block/non-solvent interaction energy has the most profound effect on the cmc, or alternatively the cmt. Unfortunately, experimental work on the PS/heptane system is virtually non-existent due to the low PS solubility. However, there are studies on the effect of pressure on A_2 for several other PS/solvent systems. Schulz and Lechner first studied the solution properties of PS in decalin, cyclohexane, chloroform and toluene in the pressure range of 1–8000 atm using classical light scattering¹⁶. Pressure caused an increase or decrease in A_2 -depending on the solvent and the temperature.

To evaluate the pressure dependence of the χ parameter in the PS/heptane system, we apply the corresponding states theory developed by Patterson¹⁹ and used by McDonald and Claesson²¹. This approach yields an expression for χ in terms of reduced temperature,

Table 3 Equation of state parameters for heptane and polystyrene

Component	T^* (K)	P^* (J cm ⁻³)	V^* cm ³ g ⁻¹	V cm ³ g ⁻¹	ν^2	τ	π
Heptane ³³	4720	435.1	1.1423	1.519			
Polystyrene ³⁷	7592	532	0.8132	0.9471			
Interaction terms					0.011175	0.37829	-0.18207


Figure 10 Pressure dependence of the PS/heptane χ parameter calculated from the corresponding states theory

pressure, and volume and several intrinsic molecular parameters as follows:

$$\chi(P, T) = c_1 \left[-\frac{\tilde{U}_1}{\tilde{T}_1} \cdot \nu^2 + \frac{1}{2} \tilde{C}_p \left\{ \tau + \frac{\tilde{P}_1 \tilde{V}_1^2}{1 + \tilde{P}_1 \tilde{V}_1^2} \cdot \pi \right\}^2 \right] \quad (7)$$

where the reduced thermodynamic quantities for the solvent are denoted with tilde superscripts. We must also find relations for the reduced configurational energy, \tilde{U}_1 , and the reduced heat capacity, \tilde{C}_p , in terms of the reduced volume, temperature and pressure. To do so, we draw from the Flory theory and assume a van der Waals model for the liquid to yield the following relations

$$\tilde{U}_1 = -\tilde{V}^{-1} \quad (8)$$

$$\frac{1}{\tilde{C}_p} = (1 - 2/3 \tilde{V}^{-1/3}) - 2 \frac{(1 - \tilde{V}^{-1/3})}{(\tilde{P} \tilde{V}^2 + 1)} \quad (9)$$

The reduced thermodynamic quantities for the solvent are described by

$$\tilde{T}_1 = \frac{T}{T^*} \quad (10)$$

$$\tilde{P}_1 = \frac{P}{P^*} \quad (11)$$

$$\tilde{V}_1 = \frac{V_1}{V_1^*} \quad (12)$$

where the starred quantities are determined from experimental values for the molar volume, thermal pressure coefficient, and the thermal expansivity of the solvent. Describing the interactions between the polymer and solvent are the parameters τ , π , and ν^2 , which are also obtained from experimental data on the pure solvent and polymer. The detailed relations between these quantities may be found in ref. 44.

The values for the reducing parameters and the intrinsic molecular parameters for n-heptane have been reported by Flory⁴⁴ and are recorded in Table 3. Flory and Hoecker have similarly determined values for PS (51 000) in the temperature range of interest by use of extrapolations from high temperature melts or high concentration solutions⁴⁷, and these are also recorded in Table 3. If we assume that these parameters are not strong functions of pressure, we can qualitatively determine the pressure dependence of the χ parameter using equation (7). McDonald and Claesson have discussed the shortcomings of this assumption but have found satisfactory agreement between theory and experiment²¹. The largest deviations from the theory would, however, be expected to occur at higher pressure where the molecular parameters may not be accurate.

Figure 10 shows the pressure dependence of the normalized χ parameter obtained from the corresponding states theory for PS/heptane at the three temperatures for which the parameters were available. An increase in pressure creates a better solvent environment for PS, as indicated by the decrease in χ . McDonald and Claesson found a similar limiting value for A_2 against pressure both experimentally and with the corresponding states theory for PS in ethyl acetate and in chloroform²¹. The decrease in the χ parameter with increasing pressure for the PS block of the PSPEP system in heptane is in qualitative agreement with our experimental observations of a decrease in cmt, or an increase in cmc, with pressure. Mean field calculations by Munch and Gast have shown that the cmc increases as the χ parameter between the core block and the solvent is decreased¹³.

Implications of the sign of the volume change upon micellization

In addition to predicting the change in the cmt with increasing pressure, our results on the pressure dependence of the χ parameter can also be used to predict the positive ΔV_{mic} at higher pressures. The implication of a positive ΔV_{mic} is that a copolymer chain displaces less volume in the dispersed state than a similar chain incorporated in a micelle. Because the PS core block undergoes the greatest change on micellization, we focus our attention on the volumetric changes of the PS block when going from a solvated state to a PS-rich environment in the micelle core. Since this is opposite to what occurs for PS mixing in heptane, we might expect the mixing volume of PS in heptane to have the opposite sign to that of ΔV_{mic} .

We use the approach of Gaeckle and Patterson¹⁹ to relate the pressure derivative of A_2 to the volume of dilution. They calculate the volume of dilution from

$$\frac{\Delta V_1}{V_1} = c^2 RT \left[- \left(\frac{\partial A_2}{\partial P} \right)_T - \beta_1 A_2 \right] \quad (13)$$

where V_1 is the molar volume of the solvent, c is the molar concentration, and β_1 is the isothermal compressibility of

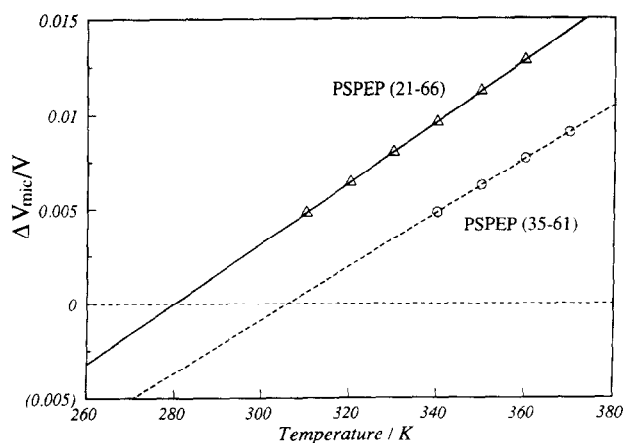


Figure 11 Temperature dependence of ΔV_{mic} in the 17–35 MPa range for both PSPEP 35/61 and PSPEP 21/66 normalized by the molar volume of the individual core blocks

the solvent. Generally, the second term in the bracket is small compared to the pressure derivative of A_2 and may be neglected. In that case, the volume of dilution has the opposite sign of $(\partial A_2/\partial p)_T$. The relation between the volume of dilution and the volume of mixing is described by

$$\frac{\Delta V_{\text{m}}}{V} = \frac{\Delta V_1 \phi_1}{V_1 \phi_2} \quad (14)$$

so that the volume of mixing will also have the opposite sign from $(\partial A_2/\partial p)_T$. Since the χ parameter for PS/heptane decreases with increasing pressure, corresponding to a positive $(\partial A_2/\partial p)_T$ we would expect that the volume of mixing would be negative. Because mixing is the reverse of the micellization process, we can then state that the contribution to ΔV_{mic} due to the change in environment of the PS block in micellization would be positive, which is consistent with the ΔV_{mic} observed experimentally.

The pressure dependence of ΔV_{mic} is similar to the pressure dependence of $(\partial A_2/\partial p)_T$ calculated from the corresponding states theory. The latter decreases in magnitude and approaches zero at high pressures. The actual values of $(\partial A_2/\partial p)_T$ at higher pressures may be inaccurate as a result of the poor approximation of the intrinsic molecular parameters in the corresponding states model at high pressures. Nevertheless, ΔV_{mic} and $(\partial A_2/\partial p)_T$ show good qualitative agreement.

Temperature dependence of the change of volume upon micellization

A temperature dependence of ΔV_{mic} is also observed from the low pressure data shown in Figure 9. Figure 11 shows the temperature dependence of ΔV_{mic} for each block copolymer in the 17–35 MPa range. We chose this pressure range for comparison because of the uncertainty of the points at atmospheric pressure for the 35/61 copolymer, for which ΔV_{mic} increases linearly with increasing temperature. Extrapolation of the data yields a ΔV_{mic} value of zero at 308 K. Similarly, ΔV_{mic} equals zero at 280 K for the 21/66 block copolymer. We can compare the temperature dependence of ΔV_{mic} with the temperature dependence of $(\partial A_2/\partial p)_T$ using equation (13). Moreover, we can compare the magnitudes of ΔV_{mic} at different temperatures by looking at the corresponding states theory shown in

Figure 10. The slopes at low pressures at 298 and 323 K show a decrease at lower temperatures indicating a lower ΔV_{mic} , but in neither case does the pressure derivative of χ go to zero.

In analogous experiments, Schulz and Lechner observed a negative $(\partial A_2/\partial p)_T$ for PS ($M_w = 10^5$) in cyclohexane at 313 K and positive values at 318 and 323 K over the pressure range from 0.1 to 40 MPa³⁸. In the PS/*trans*-decalin system they observed a negative $(\partial A_2/\partial p)_T$ from 288 to 308 K and a positive $(\partial A_2/\partial p)_T$ value at 313 K. Gaeckle and Patterson explain these observations in terms of free volume differences between polymer and solvent as a function of temperature¹⁹. At higher temperatures, the free volume effects may dominate to give a negative ΔV_1 , but at lower temperatures these effects may be less important. These observations reveal a positive ΔV_1 at higher temperatures and a negative ΔV_1 at lower temperatures. This would correspond to a positive ΔV_{mic} at higher temperatures and a negative ΔV_{mic} at lower temperatures, exactly as is seen in our experiments.

The dynamic light scattering results of Figure 1 provide complementary information to this thermodynamic discussion. We have seen that ΔV_{mic} is negative for the 35/61 block copolymer and positive for the 21/66 block copolymer at room temperature. The decrease in free chain concentration with increasing pressure in the 35/61 block copolymer micelle solution is then equilibrated with a less dense micellar phase. To decrease the osmotic pressure of the micelle phase, the corona chains will stretch to increase the micelle size, in spite of a possible decrease in overall aggregation number. This effect has been captured by the mean-field calculations of Munch and Gast¹³ on a model block copolymer micelle system, where a decrease in the cmc is accompanied by an increase in the corona size and the overall micelle size. In the case of the 21/66 block copolymer, the increase in pressure is accompanied by an increase in the free chain concentration. This causes the corona chains to contract to match osmotic pressures with the more concentrated background phase. Moreover, our observation that the micelle size changes are greatest at the lowest pressures is consistent with the idea that the micelle size is correlated with ΔV_{mic} .

As a cautionary note, we recognize that ΔV_{mic} may include other volume terms that may be temperature-dependent. One other such effect that may manifest itself in a temperature dependence of the volume change upon micellization may be the loss of freedom associated with the geometric constraint of a narrow curved interface between the blocks. This entropic penalty may be uncovered through the Maxwell relation

$$\left(\frac{\partial \Delta V_{\text{mic}}}{\partial T}\right)_P = -\left(\frac{\partial \Delta S_{\text{mic}}}{\partial P}\right)_T \quad (15)$$

From our data, we expect that the entropy of micellization will become more negative as the pressure is increased, possibly due to a more highly ordered micelle phase, or to a narrowing of the micelle interfacial region. This latter observation has previously been made by Turro and Chung⁴⁸, who used a fluorescence probe technique to study the structural changes incurred as the pressure on a polyol surfactant was increased.

Molecular weight dependence

It is interesting to compare the behaviour of the two different block copolymers. Table 2 shows that the ΔV_{mic}

for the 21/66 block copolymer is larger than that for the 35/61 block copolymer. This is contrary to our suggestion that the PS mixing volume is the dominant factor in determining ΔV_{mic} . One possible explanation for this is the difference in PS conformation in the dispersed phase. The polymer with the larger PS block may be able to tightly coil itself in a unimolecular micelle, thereby minimizing contact with the solvent. On the other hand, the shorter PS block polymer may exist in a somewhat more extended state or be more exposed to the heptane solvent. This increased solvent contact may manifest itself in a higher mixing volume for the PS block or a higher ΔV_{mic} for the micelle.

McDonald and Claesson also looked at the effect of the molecular weight on the volume of dilution for high molecular weight PS in ethyl acetate at 24°C²¹. The volume of dilution was independent of molecular weight above $M_w = 4 \times 10^5$, but V_1 increased by a factor of two for $M_w = 1.6 \times 10^5$. This again would indicate that molecular weight may play an important role in the volumetric properties of the micellization process in block copolymers. Saeki *et al.*⁴⁹ measured the pressure dependence of the upper critical solution temperature for the PS/cyclohexane system and concluded that the excess volumetric properties are not only molecular weight-dependent, but can also change sign with molecular weight.

SUMMARY

We believe that this is the first report on the pressure dependence of the cmt for a block copolymer micelle system in organic solvents. We have determined that the excimer emission band energy is a sensitive measure of local environment around excimer forming sites in the PS micelle core, and we have utilized this sensitivity to monitor the cmt as a function of pressure. These measurements were in excellent agreement with light scattering measurements. A simple thermodynamic argument involving a positive volume change upon micellization was used to characterize the decrease in cmt as the pressure was increased. We explained the decrease in the Flory interaction parameter with increasing pressure through application of Patterson's corresponding states theory. Although this purely enthalpic argument gives qualitatively correct results, entropic changes associated with interface narrowing, shape changes and changes in core solvent content are also possible and should be included in a more extended treatment.

ACKNOWLEDGEMENTS

This work was supported by the Polymers Program of the NSF Division of Materials Research and by Shell Development Company. We thank Dr Dale Handlin of Shell Development Co. for the block copolymer samples and the molecular weight characterization and Dr Robert Ju for his assistance with the dynamic light scattering measurements and data analysis.

REFERENCES

- Duval, M. and Picot, C. *Polymer* 1987, **28**, 793
- Bahadur, P., Sastry, N. V., Marti, S. and Riess, G. *Coll. Surf.* 1985, **16**, 337
- Candau, F., Heatley, R., Price, C. and Stubbersfield, R. B. *Eur. Polym. J.* 1984, **20**, 685
- Mandema, W., Emeis, C. A. and Zeldenrust, H. *Makromol. Chem.* 1979, **180**, 2163
- Yeung, A. S. and Frank, C. W. *Polymer* 1990, **31**, 2089, 2101
- Higgins, J. S., Dawkins, J. V., Maghami, G. G. and Shakir, S. A. *Polymer* 1986, **27**, 931
- Tuzar, Z., Plestil, J., Konak, C., Hlavata, B. and Sikora, A. *Makromol. Chem.* 1983, **184**, 2111
- Bednar, B., Devaty, J., Koupalova, B., Kralicek, J. and Tuzar, Z. *Polymer* 1984, **25**, 1178
- Duval, M. and Picot, C. *Polymer* 1987, **28**, 798
- Tuzar, Z. and Kratochvil, P. *Makromol. Chem.* 1972, **160**, 301
- Noolandi, J. and Hong, K. M. *Macromolecules* 1983, **16**, 1443
- Leibler, L., Orland, H. and Wheeler, J. C. *J. Chem. Phys.* 1983, **79**, 3550
- Munch, M. R. and Gast, A. P. *Macromolecules* 1988, **21**, 1360
- Price, C., Kendall, K. D., Stubbersfield, R. B. and Wright, B. *Poly. Commun.* 1983, **24**, 326
- Ver Strate, G. and Struglinski, M. J. *ACS Symp. Ser.* 1991, **462**, 256
- Schulz, G. V. and Lechner, M. *J. Polym. Sci. A-2* 1970, **8**, 1885
- Lechner, M. and Schulz, G. V. *Eur. Polym. J.* 1970, **6**, 945
- Patterson, D. *Macromolecules* 1969, **2**, 672
- Gaekle, D. and Patterson, D. *Macromolecules* 1972, **5**, 136
- Prigogine, I., Mathod, V. and Bellemans, A. 'The Molecular Theory of Solutions', North Holland, Amsterdam, 1957.
- McDonald, C. J. and Claesson, S. *Chem. Scr.* 1976, **9**, 36
- Roots, J. and Nystrom, B. *Macromolecules* 1982, **15**, 553
- Freeman, B. D., Soane, D. S. and Denn, M. M. *Macromolecules* 1990, **23**, 245
- Fitzgibbon, P. D. and Frank, C. W. *Macromolecules* 1981, **14**, 1650
- Kratochvil, P. 'Classical Light Scattering From Polymer Solutions', Elsevier, Amsterdam, 1987
- Provencher, S. W. *Comput. Phys. Commun.* 1982, **27**, 213
- Provencher, S. W. *Comput. Phys. Commun.* 1982, **27**, 229
- Yakhot, V., Cohen, M. D. and Ludmer, Z. *Adv. Photochem.* 1979, **11**, 489
- Watanabe, A. and Matsuda, M. *Macromolecules* 1985, **18**, 273
- Tuzar, Z. and Kratochvil, P. *Adv. Coll. Int. Sci.* 1976, **6**, 201
- Phillips, J. N. *Trans. Faraday Soc.* 1955, **51**, 561
- Tuddenham, R. F. and Alexander, A. E. *J. Phys. Chem.* 1962, **66**, 1839
- Osugi, J., Sato, M. and Ifuku, N. *Rev. Phys. Chem. Jpn* 1968, **38**, 58
- Tanaka, M., Kaneshina, S., Shin-no, K., Okajima, T. and Tomida, T. *J. Coll. Sci. Int. Sci.* 1974, **46**, 1974
- Kaneshina, S., Tanaka, M., Tomida, T. and Matuura, R. *J. Coll. Sci. Int. Sci.* 1974, **48**, 450
- Vikingstad, E., Skauge, A. and Hoiland, H. *J. Coll. Sci. Int. Sci.* 1979, **72**, 59
- Brun, T. S., Hoiland, H. and Vikingstad, E. *J. Coll. Sci. Int. Sci.* 1978, **63**, 89
- Hamann, S. *Rev. Phys. Chem. Jpn* 1978, **48**, 60
- Offen, H. W. *Rev. Phys. Chem. Jpn* 1980, **50**, 97
- Offen, H. W. and Turdley, W. D. *J. Coll. Sci. Int. Sci.* 1982, **87**, 442
- Wong, P. T. T. and Mantsch, H. H. *J. Chem. Phys.* 1983, **78**, 7362
- Kaneshina, S., Shibata, O., Makamura, M. and Tanaka, M. *Coll. Surf.* 1983, **6**, 73
- Hara, K., Suzuki, H. and Takisawa, N. *J. Phys. Chem.* 1989, **93**, 3710
- Flory, P. J., Orwoll, R. A. and Vrij, A. *J. Am. Chem. Soc.* 1964, **86**, 3507
- Eichinger, B. E. and Flory, P. J. *Trans. Faraday Soc.* 1968, **64**, 2035
- Eichinger, B. E. and Flory, P. J. *Trans. Faraday Soc.* 1968, **64**, 2066
- Hoecker, H., Blake, G. J. and Flory, P. J. *Trans. Faraday Soc.* 1971, **67**, 2258
- Turro, N. J. and Chung, C. *Macromolecules* 1984, **17**, 2123
- Saeki, S., Kuwahara, N., Nakata, M. and Kaneko, M. *Polymer* 1975, **16**, 445